Co-published by
Institute of Fluid-Flow Machinery
Polish Academy of Sciences
Committee on Thermodynamics and Combustion
Polish Academy of Sciences

http://www.imp.gda.pl/archives-of-thermodynamics/

Energy consumption prediction and energy-saving retrofit design for office buildings in climate adaptation

Yining Shen

Department of Architecture Engineering, Shijiazhuang College of Applied Technology, 226/227 Tianning Road, Shijiazhuang 050800, China
Author email: 2017010854@sjzpt.edu.cn

Received: 27.06.2025; revised: 15.10.2025; accepted: 08.12.2025

Abstract

In order to accurately predict the energy consumption and design energy-saving retrofits for office buildings, this study proposes a climate adaptation-based energy consumption prediction method by combining depthwise separable convolution and frequency-guided two-dimensional tensorisation algorithm. A multi-objective optimisation retrofit design model is then constructed using the non-dominated sorting genetic algorithm III and ideal point method. Experimental results show that the prediction method achieves the highest accuracy of 96.3% and the lowest error rate of 5.9% under various climate conditions, outperforming comparison algorithms. In practical applications, the retrofit design model responds in as little as 7.3 s and consumes a minimum memory of 189 MB. With a 30% increase in electricity prices, the payback period is only 6.05 years, and the carbon reduction rates for air conditioning and lighting are 59.9% and 58.6%, respectively. The results indicate that the proposed model provides a design solution with high prediction accuracy, robustness and cost-effectiveness, improving the feasibility of office buildings' low-carbon transformation.

Keywords: Depthwise separable convolution; Frequency-guided two-dimensional tensorisation algorithm; Multi-objective optimisation; Energy-saving; Energy consumption prediction

Vol. 47(2026), No. 1, 195–204; doi: 10.24425/ather.2026.158669

Cite this manuscript as: Shen, Y. (2026). Energy consumption prediction and energy-saving retrofit design for office buildings in climate adaptation. *Archives of Thermodynamics*, 47(1), 195–204.

1. Introduction

With the increasing severity of global climate change and the frequent occurrence of extreme weather events, energy conservation and emission reduction have become urgent issues facing the world. Office buildings, as major contributors to urban energy consumption, account for approximately 40% of total urban energy use. It is essential to retrofit these buildings to reduce carbon emissions [1]. Before implementing energy-saving retrofits in office buildings, energy consumption prediction is required to develop targeted retrofit plans. However, traditional energy consumption prediction methods often rely on static climate parameters and fail to account for inter-periodic climate variations. This results in significant deviations between predicted and actual outcomes, leading to suboptimal retrofit effects [2,3]. The frequency-guided two-dimensional tensorisation algorithm (FGTTA) improves the energy consumption prediction accuracy under dynamic climate conditions by considering both intra-seasonal and inter-seasonal variations through higher-order tensor decomposition and feature mapping [4]. Depthwise separable convolution (DSC) reduces computational complexity while maintaining comprehensive feature extraction [5]. Therefore, this study combines depthwise separable convolution and frequency-guided two-dimensional tensorisation algorithm to propose a climate adaptation-based energy consumption prediction algorithm, named DSC-FGTTA.

Nomenclature

Abbreviations and Acronyms

AECOSIM – architecture, engineering, construction and operations integrated simulation model
BIM – building information modelling
DSC – depthwise separable convolution
ECP-RD – energy consumption prediction and retrofit design
FGTTA – frequency-guided two-dimensional tensorisation algorithm
IPM – ideal point method
IR – inverted residuals
MEA-BP – mind evolutionary algorithm-back propagation neural network
NSGA-III – third-generation non-dominated sorting genetic algorithm
NZEB – net zero energy building
PSO-SVM – particle swarm optimisation-support vector machine
TFEU – tensor feature extraction unit
XAI – explainable artificial intelligence

Multi-objective optimisation algorithms can simultaneously address energy saving, long-term costs and indoor comfort, maximising the benefits and optimising the resource allocation of retrofit plans [6,7]. Based on DSC-FGTTA, this study introduces the third-generation non-dominated sorting genetic algorithm (NSGA-III) and ideal point method (IPM) to design energy-saving retrofit plans for office buildings, constructing an energy consumption prediction and retrofit design (ECP-RD) model that considers long-term costs and indoor comfort. This model aims to couple data-driven methods with physical mechanisms, such as the thermodynamics of building envelope structures and the dynamic interaction process between the indoor environment and external climate, in order to improve the accuracy of predictions. It provides decision-makers with a clear and interpretable energy-saving transformation solution, based on the principle of energy transfer and conversion.

Compared with existing research in the field of building energy consumption prediction methods, the main innovation of this study lies in: (1) Combining depthwise separable convolution with frequency guided two-dimensional tensorisation algorithm to propose a climate adaptive energy consumption prediction model DSC-FGTTA, which effectively captures multi period dynamic climate characteristics and overcomes the shortcomings of traditional static models in cross period trend analysis; (2) At the same time, NSGA-III multi-objective optimisation and ideal point method were introduced to construct an energy-saving renovation design (ECP-RD) model that integrates energy consumption, cost and comfort, achieving integrated optimisation from prediction to renovation strategy generation, significantly improving the scientificity and practicality of decision-making.

2. Related works

The frequency-guided two-dimensional tensorisation algorithm, due to its structured data-carrying capacity and flexible mathematical operations, has become a core tool in data processing. Experts and scholars worldwide have explored and studied its applications. For example, the research team led by Zheng proposed a semi-blind thick cloud removal method based on the two-dimensional tensor algorithm, solving the issues of incomplete information recovery and colour distortion in traditional thick cloud removal methods in remote sensing image processing. The final experimental results verified the effectiveness of the method [8]. Wang et al. [9], in order to address the inefficiency caused by high computational and storage complexity in modelling high-dimensional nonlinear autoregressive exogenous systems, proposed a new hybrid modelling and recognition algorithm by combining two-dimensional tensor networks and recursive algorithms. Numerical experiments confirmed the superiority of this algorithm.

The depthwise separable convolution, due to its low computational and parameter requirements and high operational efficiency, has become a favoured method for scholars across various fields. For instance, Asker et al. [10] addressed the issues of large parameter quantities and insufficient feature representation in classifying hyperspectral images using a traditional convolutional neural network. By utilising DSC in the network architecture, they reduced the number of parameters while maintaining both classification accuracy and computational complexity. Due to the inability of standard convolutional networks to accurately classify fisheye freshness based on subtle features, Prasetyo's research team enhanced the model's ability to express subtle features through an improved DSC, thereby improving the accuracy of fisheye freshness classification [11]. Multi-objective optimisation algorithms can simultaneously balance multiple optimisation objectives, making them highly practical in real-world production and daily life. As a result, many scholars have explored the application of these algorithms. For example, to address the problem of traditional feature selection methods struggling to balance the efficiency and accuracy of feature extraction in data processing, Abdollahzadeh et al. [12] proposed a multi-objective hybrid optimisation algorithm, which achieved improvements in both efficiency and accuracy.

Accurate building energy consumption prediction is of significant importance for building retrofitting. Therefore, experts and scholars worldwide have conducted extensive research on energy consumption prediction for buildings. For instance, to address the issue of data sparsity in building energy consumption prediction, Qiao et al. [13] improved the traditional prediction method's feature extraction approach using multivariate packaging methods. Experimental results demonstrated the good accuracy and robustness of this method. Buturache et al. [14] tackled the issue of low historical data utilisation in practical building energy consumption predictions by integrating data preprocessing strategies and hyperparameter optimisation techniques. They developed a method capable of balancing trade-offs, and their final experiments showed that the method could balance the performance and flexibility in building energy consumption prediction.

Energy-saving retrofitting of buildings not only alleviates energy and environmental pressures but also has economic significance. As a result, experts and scholars around the world have conducted in-depth research on this topic. For example, Li

et al. [15] addressed the high energy consumption in mountainous campus buildings by applying computational fluid dynamics wind environment simulation technology and ergonomic programming systems combined with composite insulation layer façade retrofitting technology. The energy-saving rate of the retrofitted campus buildings reached 24%. Borràs et al. [16], through experiments, compared the energy-saving effects of only retrofitting the roof versus retrofitting the entire thermal envelope of buildings, revealing the impact of building roofs on energy savings. This study provides more reference for selecting energy-saving retrofit solutions in buildings.

In conclusion, while there have been some improvements in the prediction accuracy of building energy consumption methods, issues such as not considering climate factors and computational complexity remain. Regarding the exploration of building energy-saving retrofit design methods, most studies still focus only on energy-saving effects, without considering costs and comfort. In light of this, the study combines FGTTA and DSC to propose a climate-adaptation-based building energy consumption prediction method that balances prediction accuracy and computational load. The energy consumption data output by the above prediction method was used as the optimisation input, and the NSGA-III multi-objective optimisation algorithm was further introduced to construct a building energy-saving renovation design model, in order to seek the optimal balance between multiple objectives. It is expected that this model will provide more practical and excellent retrofit solutions for building energy-saving retrofits.

3. Climate-adaptive energy prediction and energy-saving model for office buildings

3.1. Design of energy consumption prediction algorithm for office buildings

For building energy consumption prediction, traditional models only analyse single-period trends, ignoring the longitudinal correlations of data across different periods. This leads to an insufficient capture of energy consumption fluctuations caused by factors such as climate, increasing the prediction error rate. This study conceptualises an office building as a dynamic thermodynamic system, whose energy consumption and comfort state fundamentally depend on the thermal performance of the building envelope, indoor and outdoor climate boundary conditions and the dynamic balance of internal thermal disturbances. The proposed mathematical architecture of the prediction and optimisation model aims to accurately describe the operating laws of this physical system and to use climate parameters as the core physical driving variables to ensure that the model output results have a solid physical foundation. The frequency-guided two-dimensional tensorisation algorithm can capture both seasonal variations within the same period and corresponding changes across different periods through its multi-layered network structure [17]. Therefore, this study uses FGTTA to extract multi-level seasonal features of energy consumption data from office buildings.

The algorithm structure is shown in Fig. 1. As shown in the figure, FGTTA consists of multiple two-dimensional tensor feature extraction units (TFEUs). Taking one two-dimensional TFEU as an example, the energy consumption data is first mapped to one-dimensional deep features. Then, the one-dimensional data is mapped to a two-dimensional space, obtaining a set of two-dimensional tensors. Convolutional neural networks perform convolution operations on the two-dimensional tensor group, which is then converted back to a one-dimensional tensor. Finally, the one-dimensional vectors are concatenated to obtain the final prediction result. The mapping of the one-dimensional energy consumption data to deep features, resulting in a one-dimensional time series, is expressed by the equation

$$X_{1\mathrm{D}}^{h} = \mathrm{TFEU}\left(X_{1\mathrm{D}}^{h-1}\right) + X_{1\mathrm{D}}^{h-1}, \tag{1}$$

where h represents the layer of TFEU, and $X_{1\mathrm{D}}^{h-1}$ and $X_{1\mathrm{D}}^{h}$ represent the input and output values. After the one-dimensional time series $X_{1\mathrm{D}}^{h-1}$ is tensorised into a two-dimensional tensor group $X_{2\mathrm{D}}^{h,i}$, convolution is applied to $X_{1\mathrm{D}}^{h-1}$, as shown in the equation

$$\hat{X}_{2\mathrm{D}}^{h,i} = \mathrm{Re\,Lu}\left\{\mathrm{BN}\left[\mathrm{Conv2D}\left(X_{2\mathrm{D}}^{h,i}\right)\right]\right\},\ i \in \{1, \ldots, k\}, \tag{2}$$

where $\mathrm{Conv2D}(\cdot)$, $\mathrm{BN}(\cdot)$, and $\mathrm{ReLu}(\cdot)$ represent the convolution layer, batch normalisation layer, and activation function layer, respectively, and $\hat{X}_{2\mathrm{D}}^{h,i}$ is the two-dimensional tensor obtained after the convolution operation. The sequence is then truncated, and the amplitude corresponding to the relative importance of the two-dimensional tensor is calculated. Based on this relative importance, the two-dimensional vector is dynamically concatenated to form a one-dimensional tensor. This process is expressed as follows

$$\begin{cases} \hat{X}_{1\mathrm{D}}^{h,i} = \mathrm{Tru}\left[\mathrm{Re\ factor}_{1,(f_i \times \tau_i)}\left(\hat{X}_{2\mathrm{D}}^{h,i}\right)\right], \ i \in \{1, \ldots, k\}, \\ \hat{A}_{f_1}^{h-1}, \ldots, \hat{A}_{f_k}^{h-1} = \mathrm{Soft\,max}\left(A_{f_1}^{h-1}, \ldots, A_{f_k}^{h-1}\right), \\ X_{1D}^{h} = \sum_{i=1}^{k} \hat{A}_{i}^{h-1} \times \hat{X}_{1\mathrm{D}}^{h,i}, \end{cases} \tag{3}$$

where $\mathrm{Tru}(\cdot)$ represents the truncation operation, $\hat{X}_{1\mathrm{D}}^{h,i}$ represents the converted one-dimensional time series, and f_i and τ_i represent the row and column numbers of the two-dimensional tensor.

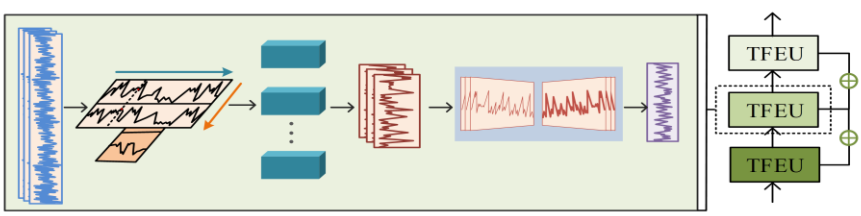

Fig. 1. Schematic diagram of FGTTA structure.

Variable A represents the amplitude strength of the frequency domain components obtained through the Fourier transform, k represents the first largest frequency domain components, $\hat{A}_{f_k}^{h-1}$ represents the amplitude weights of $A_{f_k}^{h-1}$ calculated by the Softmax function, and X_{1D}^{h} represents the final concatenated one-dimensional sequence.

The frequency-guided two-dimensional tensorisation algorithm improves the accuracy of long-term energy consumption prediction by analysing both single-period and cross-period energy trends. However, the time complexity increases, affecting the prediction efficiency. The depthwise separable convolution reduces computation and model parameters while maintaining feature extraction performance through depthwise and pointwise convolutions [18,19]. The inverted residuals (IR) network can not only overcome the data loss limitation of traditional residual networks, but also reduce the computational resources required. Therefore, this study proposes a feature extraction network combining DSC and IR, named DSC-IR, as shown in Fig. 2.

As shown in Fig. 2, the DSC-IR network consists of multiple convolution stages and pooling layers. The convolution stages are composed of inverted residual modules, which first increase the channel count through a convolution layer, then use depthwise separable convolutions to extract feature map features, and finally reduce the channel count through another convolution layer. By using different numbers of inverted residual modules at different stages, features at various levels and scales can be captured. After efficiently extracting features through the convolution stages, the pooling layers further reduce the dimensions of the feature maps. The depthwise separable convolution extracts spatial features from each channel, with each channel's depthwise convolution represented by the equation

$$\hat{G}_{k,l,m} = \sum_{i,j} \hat{k}_{i,j,m} \cdot F_{k+i-1,l+j-1,m}, \quad (4)$$

where $\hat{k}$ represents the depth convolution kernel of size $D_K \times D_K \times M$, m in $\hat{k}_{i,j,m}$ represents the m-th convolution kernel, and m in $F_{k+i-1,l+j-1,m}$ and $\hat{G}_{k,l,m}$ represents the m-th channel in the input feature and output feature, respectively. The computational cost of depth convolution is expressed as

$$C_1 = D_K \times D_K \times M \times D_F \times D_F, \quad (5)$$

where M represents the number of input channels and D_F represents the width and height of the input feature map. After extracting spatial features from the feature map through depthwise convolution, a pointwise convolution is applied to fuse the features, forming new features. The computational cost of the final depthwise separable convolution after pointwise convolution is expressed as

$$C_2 = D_K \times D_K \times M \times D_F \times D_F + N \times M \times D_F \times D_F, \quad (6)$$

where N represents the number of output channels.

The DSC-IR network effectively reduces computation while maintaining stable feature extraction performance, balancing both performance and efficiency. To further enhance the algorithm's predictive performance, the study replaces the convolutional neural network part of the two-dimensional tensorisation algorithm with the deep separable inverted residual network,

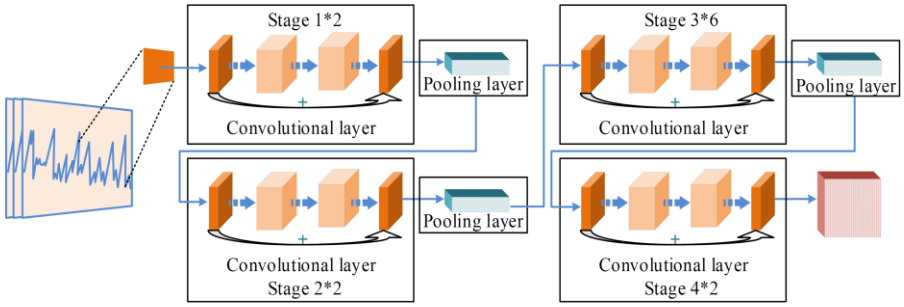

Fig. 2. The DSC-IR network structure.

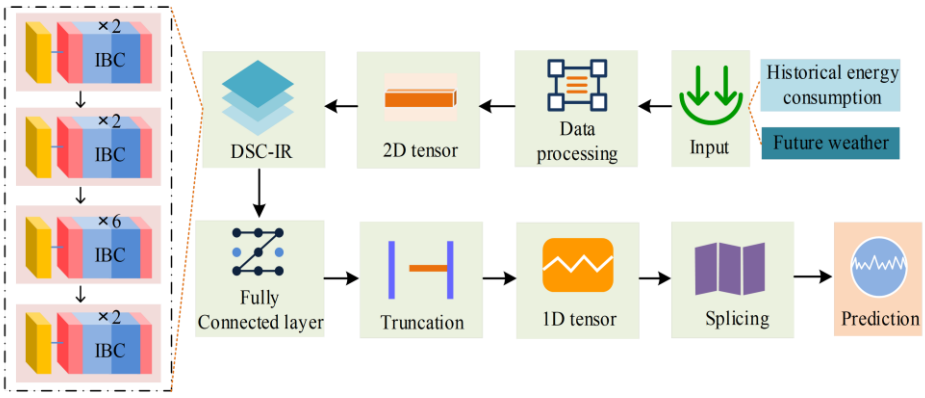

Fig. 3. The DSC-FGTTA flowchart.

proposing a DSC-FGTTA-based energy prediction algorithm for office buildings.

As shown in Fig. 3, which illustrates the prediction flow, in the DSC-FGTTA, historical energy consumption and future weather data are input and standardised to eliminate scale differences, then converted into two-dimensional spatial tensors. Next, the DSC-IR module performs multi-stage convolution and pooling operations to extract features and reduce dimensions. The processed feature data is returned to the fully connected layer of FGTTA, where different features are integrated to obtain a global description of the data. The energy consumption features are then truncated to form a fixed-length one-dimensional tensor, and weighted concatenation is applied to construct the final prediction sequence. Finally, future energy consumption is predicted based on the final tensor sequence. DSC-FGTTA effectively captures short-term and long-term energy consumption trends from historical data, enabling accurate predictions of seasonal fluctuations.

3.2. Prediction and energy-saving model based on multi-objective optimisation algorithm

After predicting the energy consumption of the target office building using DSC-FGTTA, it is necessary to design a targeted renovation plan to minimise future energy consumption and achieve energy savings. However, the renovation of office buildings does not only consider energy consumption, but also takes into account long-term costs and indoor comfort. NSGA-III can continuously approach the optimal solution by evaluating fitness and eventually obtain a set of non-dominated pre-optimal solutions [20]. Therefore, this study uses NSGA-III to determine the optimal renovation plan based on the prediction results from DSC-FGTTA, as illustrated in Fig. 4. As shown in the figure, NSGA-III first defines the target problem as a reference point, then initialises a set of random solutions and calculates their fitness. Afterwards, a subset of high-fitness random solutions is selected as parents. These parent solutions undergo crossover to generate new solutions, and mutation operations are applied to introduce additional solutions. The newly generated and introduced solutions are added to the current solution set. The iteration process continues until the maximum number of iterations is reached or the solution and fitness meet the preset criteria; then the iteration stops, and the final results are output. This

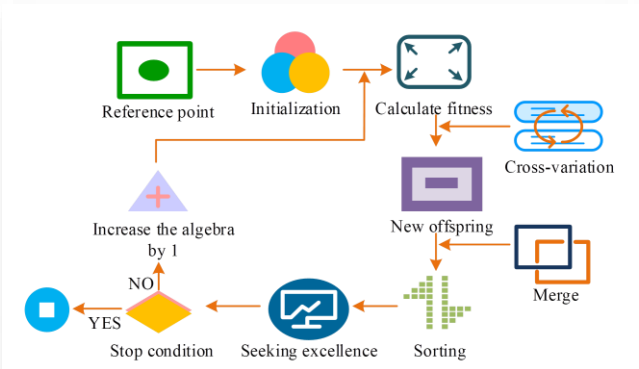

Fig. 4. The NSGA-III implementation flowchart.

study sets the maximum number of iterations to 200, and the preset convergence threshold is that the improvement of the optimal solution of the population within 20 consecutive generations is less than 0.0001. If the conditions are not met, fitness evaluation continues until the stopping conditions are reached. In the NSGA-III process, starting from the physical characteristics of the building, the energy consumption predicted by DSC-FGTTA, as well as the average predicted dissatisfaction and renovation cost determined by building thermal engineering and human thermal comfort theory, are jointly set as optimisation objectives.

As shown in the equation, the objective function is formed by the building energy consumption ($e_c(\bar{x})$), average predicted dissatisfaction ($R_{\mathrm{D}}(\bar{x})$) and renovation cost ($c(\bar{x})$):

$$G(\bar{x}) = G[(e_c(\bar{x}), R_{\mathrm{D}}(\bar{x}), c(\bar{x}))], \tag{7}$$

where $\bar{x}$ represents the optimisation variable. The study uses the average thermal sensation index to evaluate average prediction dissatisfaction, which is expressed as follows:

$$R_{\mathrm{D}} = \frac{1}{n}\sum_{i=1}^{n} \bar{R}_{\mathrm{D},i}, \tag{8}$$

where n represents the number of thermal zones in the target building and $\bar{R}_{\mathrm{D},i}$ stands for the average predicted dissatisfaction with the thermal environment. The predicted renovation cost is expressed as follows:

$$c = \frac{1}{A}\sum_{i=1}^{i} C_i = \frac{1}{A}\sum_{i=1}^{i} A_i \times c_{p,i}, \tag{9}$$

where C_i and A_i denote the incremental renovation cost and renovation area for each part of the building, respectively, and $c_{p,i}$ is the unit area cost of renovation materials. Additionally, to ensure that all design parameters comply with relevant standards, constraints are applied:

$$\begin{cases} {x^1}_{\min} < {x^1}_i < {x^1}_{\max} \\ {x^2}_{\min} < {x^2}_i < {x^2}_{\max} \\ {x^3}_{\min} < {x^3}_i < {x^3}_{\max} \end{cases}, \tag{10}$$

where ${x^1}_i$, ${x^2}_i$, and ${x^3}_i$ represent building energy consumption, dissatisfaction and renovation cost, respectively, and ${x^1}_{\min}$, ${x^2}_{\min}$, and ${x^3}_{\min}$ represent the lower limits of design parameters, while ${x^1}_{\max}$, ${x^2}_{\max}$, and ${x^3}_{\max}$ represent the upper limits of design parameters. The optimal solution set obtained through NSGA-III includes several equally valid renovation methods. However, in practical applications, only one renovation plan is typically chosen. Therefore, after obtaining the optimal solution set from NSGA-III, it is necessary to select the best solution as the final renovation plan. The ideal point method evaluates the solutions by comparing the difference between each solution and the ideal point, thus selecting the optimal solution [21].

The study adopts the IPM as the multi-objective decision-making method, combined with NSGA-III to form the optimal renovation plan determination method, named NSGA-III-IPM. The implementation process of this method is shown in Fig. 5. As seen from the figure, the NSGA-III-IPM first defines the objective and constraint functions. The study uses building energy

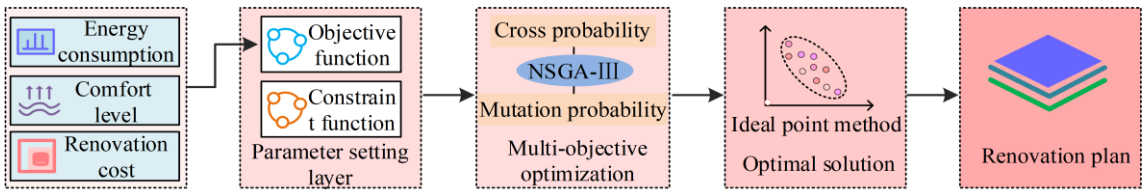

Fig. 5. The NSGA-III-IPM flowchart.

consumption, comfort and renovation cost as optimisation objectives. Then, NSGA-III is used to obtain the feasible optimal solution set. The best solution is then selected from the set of alternative optimal solutions to form the target building's renovation plan. The difference between each alternative optimal solution and the ideal solution is determined using the Euclidean distance:

$$U_n = \left[\left(\frac{\eta_{\text{Pareto}} - \eta_{\text{E}_{\text{point}}}}{\eta_{E_{point}}}\right)^2 + \left(\frac{Z_{\text{Pareto}} - Z_{\text{E}_{\text{point}}}}{Z_{\text{E}_{\text{point}}}}\right)^2\right]^{\frac{1}{2}}, \quad (11)$$

where $(\eta_{\text{Pareto}}, Z_{\text{Pareto}})$ and $(\eta_{\text{E}_{\text{point}}}, Z_{\text{E}_{\text{point}}})$ represent the coordinates of the alternative optimal solution (a Pareto optimal solution) and the ideal point. After calculating the distance between all solutions in the optimal solution set and the ideal solution, the solution closest to the ideal solution is selected:

$$U_{\text{opt}} = \min(U_n), \quad (12)$$

where U_{opt} denotes the final selected optimal solution. Finally, this study captured the dynamic physical response of buildings to external climate using the DSC-FGTTA and utilised the NSGA-II-IPM to seek the optimal solution while satisfying multiple physical and comfort constraints, thus forming a complete office building renovation design model (i.e. ECP-RD) from physical mechanism analysis to optimisation decision-making.

The overall framework of the ECP-RD model is shown in Fig. 6. In the ECP-RD model, energy consumption prediction is performed by DSC-FGTTA to extract features from historical energy consumption data and future weather, and climate-adapted energy consumption prediction results are obtained based on these features. The predicted energy consumption values are then used as one of the optimisation objectives in the renovation design part, along with comfort and renovation cost, forming the optimisation function. The NSGA-III is then applied to obtain the optimal solution set. Finally, IPM is used to determine the solution closest to the ideal solution as the optimal solution, which is the final renovation plan.

4. Performance validation of the ECP-RD energy prediction and retrofit design model

4.1. Performance validation of the DSC-FGTTA algorithm

To evaluate the energy conservation and retrofit design model proposed in this study, both algorithm performance verification experiments and practical application experiments were conducted to assess the building energy consumption prediction and renovation design performance. The comparative algorithms used in the algorithm performance verification experiments were mind evolutionary algorithm-back propagation neural network (MEA-BP), explainable artificial intelligence (XAI) and particle swarm optimisation-support vector machine (PSO-SVM). The comparative models used in the practical application experiments were building information modelling (BIM), net zero energy building (NZEB), and architecture, engineering, construction, and operations integrated simulation model (AECOSIM).

The study selected an office building in Chengdu as the target object. This building consists of 15 floors, with a standard floor height of 3 m, and integrates commercial, office and hotel functions. It uses a split air-conditioning system. The experiment used the Building Energy and Climate Database (BECD) as the dataset, which includes basic building data, equipment system information, and historical weather records. The experimental environment is shown in Table 1.

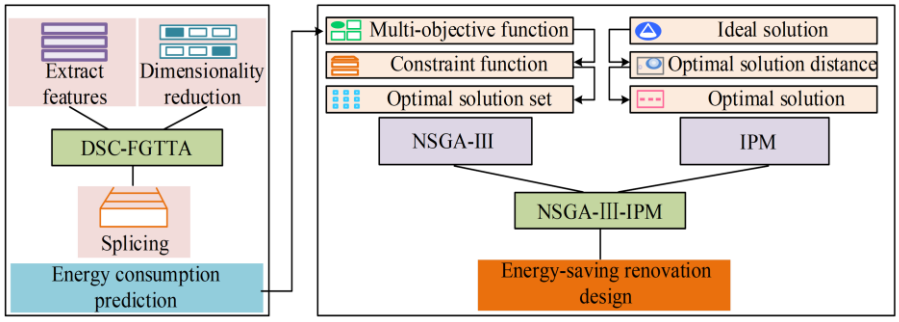

Fig. 6. The ECP-RD model structure.

Table 1. Experimental environment and configuration parameters.

Parameter	Configuration
CPU	AMD Ryzen 5
Memory	32GB
IDE	VS Code
Operating system	Windows 10
Programming language	Python 4.0
GPU	NVIDIA RTX 3090

Based on the experimental environment, the study first conducted a comparison experiment on the electrical consumption prediction methods. The experimental results are shown in Fig. 7.

As shown in Fig. 7a, when the target is the building's summer electricity consumption, the prediction accuracy of MEA-BP was 93.2%, while XAI and PSO-SVM had prediction accuracies of 91.3% and 89.5%, respectively. The prediction accuracy of DSC-FGTTA was 95.6%. As depicted in Fig. 7b, for the winter electricity consumption prediction experiment, the prediction accuracies of MEA-BP, XAI, PSO-SVM and DSC-FGTTA were 94.1%, 92.5%, 90.3% and 96.3%, respectively. From these experimental results, it can be concluded that DSC-FGTTA demonstrated higher accuracy in predicting building energy consumption across different climates, indicating that the method can adapt to dynamic climate changes. To further verify the robustness of the energy consumption prediction method, the study conducted an experiment to assess the prediction error rate under extreme weather conditions. The results are presented in Fig. 8.

As shown in Fig. 8a, during extremely hot weather, the highest and lowest error rates for the MEA-BP method were 20.6% and 15.8%, respectively. For XAI, the highest and lowest error rates were 23.4% and 15.1%, respectively. The highest and lowest error rates for PSO-SVM were 15.9% and 13.8%, respectively. For DSC-FGTTA, the highest and lowest error rates were 7.2% and 5.9%, respectively. According to Fig. 8b, during extreme weather with continuous rainfall, the highest error rates for MEA-BP and XAI were 18.1% and 23.8%, with the lowest error rates at 14.8% and 19.1%, respectively. The highest and lowest error rates for PSO-SVM were 14.9% and 12.1%, respectively. The highest and lowest error rates for DSC-FGTTA were 9.8% and 6.9%, respectively. From these data, it can be observed that under both extreme weather conditions, the prediction error rates for DSC-FGTTA remained below 10%, outperforming the comparative models. This experiment demonstrated that the DSC-FGTTA energy consumption prediction method has high prediction accuracy and excellent robustness.

4.2 Practical application of the ECP-RD model

The validation experiment of the DSC-FGTTA energy consumption prediction algorithm confirmed the high prediction accuracy and excellent robustness of the algorithm when applied to climate adaptation. It demonstrated that the DSC-FGTTA energy consumption prediction algorithm could provide a reliable

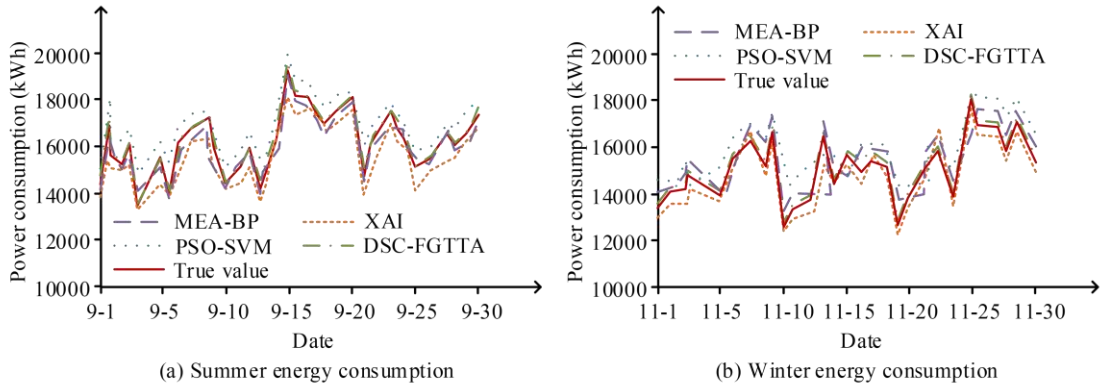

Fig. 7. Results of the electrical consumption prediction experiment.

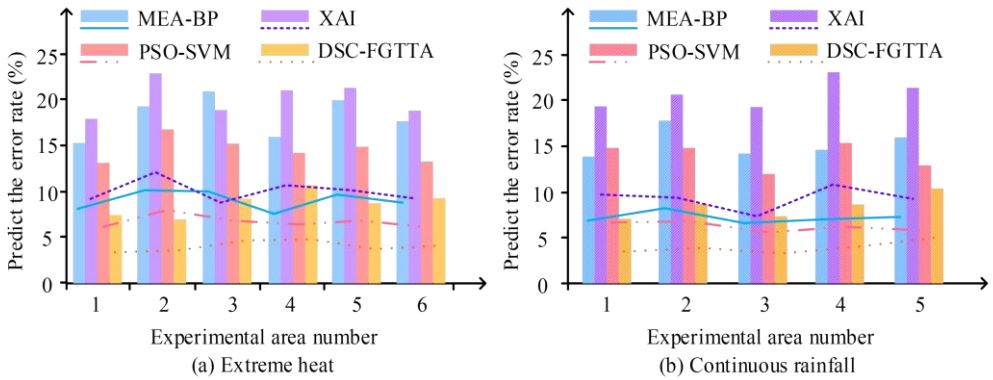

Fig. 8. Prediction error rate under extreme weather.

data source for the ECP-RD model. To further verify the practical application performance of the ECP-RD model in building energy-saving renovation design, the study first conducted experiments on the response time and memory usage of the model to evaluate its practicality. The experimental results are shown in Fig. 9.

As seen in Fig. 9a, in the response time experiment, the fastest response time for NZEB was 15.1 s, with an average response time of 15.3 s. For BIM, the fastest and average response times were 9.9 s and 11.3 s, respectively, whereas for AECOSIM, these response times were 10.4 s and 13.6 s, respectively. For the ECP-RD model proposed by the study, the fastest and average response times were 7.3 s and 10.2 s, respectively. As shown in Fig. 9b, in the memory usage experiment, the average memory usage for NZEB, AECOSIM and BIM during operation was 358 MB, 326 MB and 223 MB, respectively, while the average memory usage for ECP-RD was 189 MB.

In summary, in both the response time and memory usage experiments, ECP-RD outperformed the other three comparative models, indicating that ECP-RD has excellent practicality. After verifying the practicality of the ECP-RD model, the study continued to assess its economic benefits. The experiment used the payback period as the performance indicator, and the experimental results are shown in Fig. 10. According to Fig. 10a, when the electricity price increase was 5%, the payback periods for NZEB, BIM and AECOSIM were 8.03 years, 6.91 years and 7.06 years, respectively. The payback period for ECP-RD was 5.73 years. When the electricity price increase was 30%, the payback periods for NZEB, BIM, AECOSIM and ECP-RD increased by 1.11 years, 0.41 years, 0.75 years and 0.32 years, respectively, compared to the 5% price increase. As shown in Fig. 10b, when the equipment degradation rate reached 50%, the payback periods for the four models were 8.94 years, 5.95 years, 7.12 years and 5.62 years, respectively.

In summary, under both electricity price increase and equipment degradation, the ECP-RD model showed the shortest payback period and the smallest increase, indicating that the renovation plan provided by ECP-RD delivers excellent economic benefits.

Finally, the study conducted experiments on the energy-saving effects of the ECP-RD model. The experimental results are shown in Fig. 11. Figures 11a and b show the carbon reduction rates for air conditioning and lighting, respectively. As shown in Fig. 11a, the average carbon reduction rates for BIM, NZEB, AECOSIM and ECP-RD were 35.6%, 28.6%, 42.6% and 59.9%, respectively. In Fig. 11b, for lighting equipment, the average carbon reduction rates for NZEB, BIM, AECOSIM and ECP-RD were 30.55%, 40.9%, 43.6% and 58.6%, respectively. These experimental results clearly demonstrate that the ECP-RD model significantly outperformed the comparative models in

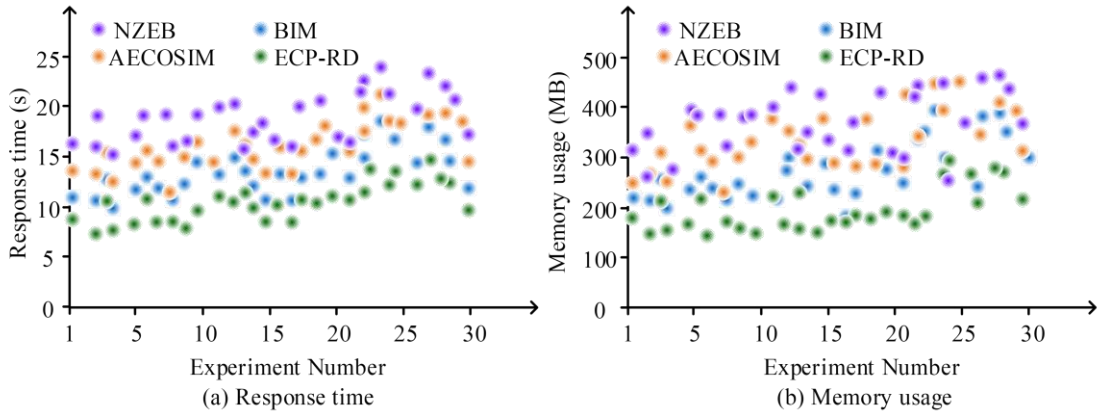

Fig. 9. Results of the response time and memory usage experiments.

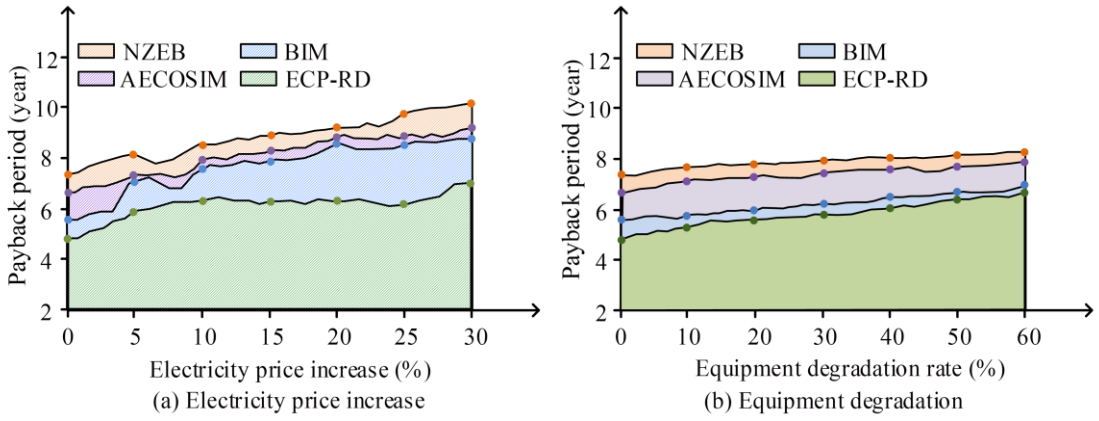

Fig. 10. Payback period experimental results.

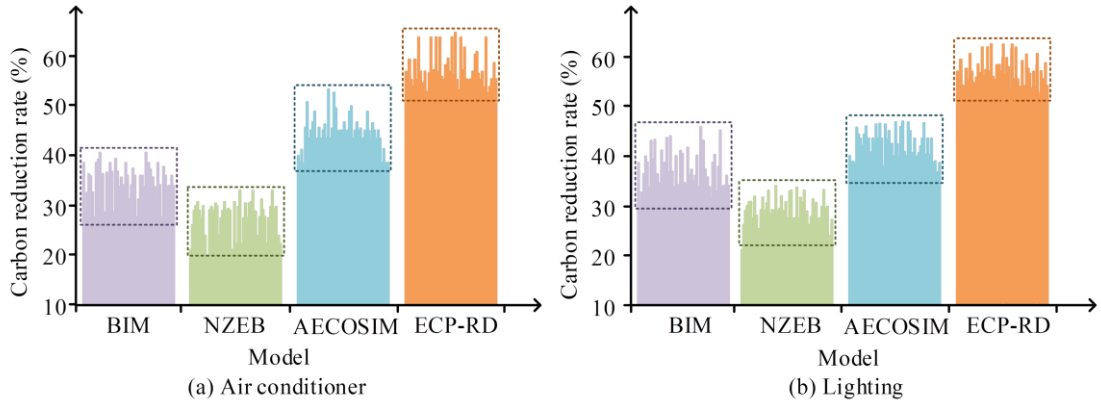

Fig. 11. Carbon reduction rate experimental results.

terms of carbon reduction, indicating that the renovation plan provided by ECP-RD can help the target building achieve substantial energy-saving effects.

6. Conclusions

In response to the energy consumption prediction and energy-saving renovation needs of office buildings facing dynamic climate changes, the study proposed a hybrid model based on depthwise separable convolution, frequency-guided two-dimensional tensorisation algorithm and multi-objective optimisation algorithms. This model integrates both building energy consumption prediction and energy-saving renovation design.

The final model performance verification results showed that the prediction accuracy for energy consumption was 95.6% in summer and 96.3% in winter, with the error rate as low as 5.9% under extreme weather conditions. These experimental data indicate that the model can accurately predict the energy consumption of the target building.

In the energy-saving renovation experiments, the model outperformed the comparative models in terms of both response time and memory usage, with an average response time of 10.2 s and memory usage of 189 MB. When the electricity price increased by 30%, the payback period was only 6.05 years, and the carbon reduction rates for air conditioning and lighting were 59.9% and 58.6%, respectively. These experimental data demonstrate that the proposed building energy consumption prediction and energy-saving renovation model has excellent prediction accuracy and robustness, helping decision-makers develop reasonable energy-saving renovation plans. This is mainly due to its core algorithm, effectively capturing and quantifying the dynamic response laws of the building thermodynamic system to external climate stimuli. Compared to pure mathematical fitting, the proposed model provides decision-makers with not only optimised results, but also clear physical mechanisms through in-depth exploration of key physical processes, such as thermal performance of building envelope structures and dynamic characteristics of air conditioning systems. However, the model currently relies heavily on the quality of historical data, and its applicability is limited in buildings with insufficient data.

References

[1] Röck, M., Balouktsi, M., & Saade, M.R.M. (2023). Embodied carbon emissions of buildings and how to tame them. *One Earth*, 6(11), 1458−1464. doi: 10.1016/j.oneear.2023.10.018

[2] Usman, A.M., & Abdullah, M.K. (2023). An assessment of building energy consumption characteristics using analytical energy and carbon footprint assessment model. *Green and Low-Carbon Economy*, 1(1), 28−40. doi: 10.47852/bonviewGLCE3202545

[3] Li, J., Zhang, C., Zhao, Y., Qiu, W., Chen, Q., & Zhang, X. (2022). Federated learning-based short-term building energy consumption prediction method for solving the data silos problem. Building Simulation. *Building Simulation*, 15(6), 1145−1159. doi: 10.1007/s12273-021-0871-y

[4] Zhang, Q., Kong, J., Jiang, M., & Liu, T. (2023). Building energy consumption prediction based on temporal-aware attention and energy consumption states. *Journal of Electrical Engineering & Technology*, 18(1), 61−75. doi: 10.1007/s42835-022-01159-3

[5] Bañuls, M.C. (2023). Tensor network algorithms: A route map. *Annual Review of Condensed Matter Physics*, 14(1), 173−191. doi: 10.1146/annurev-conmatphys-040721-022705

[6] Nguyen, X.T., & Tran, G.S. (2024). Hyperspectral image classification using an encoder-decoder model with depthwise separable convolution, squeeze and excitation blocks. *Earth Science Informatics*, 17(1), 527−538. doi: 10.1007/s12145-023-01181-7

[7] Sharma, S., & Kumar, V. (2022). A comprehensive review on multi-objective optimization techniques: Past, present and future. *Archives of Computational Methods in Engineering*, 29(7), 5605−5633. doi: 10.1007/s11831-022-09778-9

[8] Zheng, W.J., Zhao, X.L., Zheng, Y.B., Lin, J., Zhuang, L., & Huang, T.Z. (2023). Spatial-spectral-temporal connective tensor network decomposition for thick cloud removal. *ISPRS Journal of Photogrammetry and Remote Sensing*, 199(1), 182−194. doi: 10.1016/j.isprsjprs.2023.04.006

[9] Wang, Y., Tang, S., & Deng, M. (2022,).Modeling nonlinear systems using the tensor network B-spline and the multi-innovation identification theory. *International Journal of Robust and Nonlinear Control*, 32(13), 7304−7318. doi: 10.1002/rnc.6221

[10] Asker, M.E. (2023). Hyperspectral image classification method based on squeeze-and-excitation networks, depthwise separable convolution and multibranch feature fusion. *Earth Science Informatics*, 16(2), 1427−1448. doi: 10.1007/s12145-023-00982-0

[11] Prasetyo, E., Purbaningtyas, R., Adityo, R.D., Suciati, N., Fatichah, C. (2022). Combining MobileNetV1 and Depthwise Separable convolution bottleneck with Expansion for classifying the

freshness of fish eyes. *Information Processing in Agriculture*, 9(4), 485−496. doi: 10.1016/j.inpa.2022.01.002

[12] Abdollahzadeh, B., & Gharehchopogh, F.S. (2022) A multi-objective optimization algorithm for feature selection problems. *Engineering with Computers*, 38(Suppl. 3), S1845−S1863.

[13] Qiao, Q., Yunusa-Kaltungo, A., & Edwards, R.E. (2022). Feature selection strategy for machine learning methods in building energy consumption prediction. *Energy Reports*, 8(1), 13621−13654. doi: 10.1016/j.egyr.2022.10.125

[14] Buturache, A.N, & Stancu, S. (2022). Building energy consumption prediction using neural-based models. *International Journal of Energy Economics and Policy*, 12(2), 30−38. doi: 10.32479/IJEEP.12739

[15] Li, Y., Chen, H., & Yu, P. (2024). Green campus transformation in smart city development: A study on low-carbon and energy-saving design for the renovation of school buildings. *Smart Cities*, 7(5), 2940−2965. doi: 10.3390/smartcities7050115

[16] Borràs, J.G., Lerma, C., Mas, Á., Vercher, J., & Gil, E. (2022). Contribution of green roofs to energy savings in building renovations. *Energy for Sustainable Development*, 71(3), 212−221. doi: 10.1016/j.esd.2022.09.020

[17] Menczer, A., & Legeza, O. (2024). Tensor network state algorithms on AI accelerators. *Journal of Chemical Theory and Computation*, 20(20), 8897−8910. doi: 10.1021/acs.jctc.4c00800

[18] Asif, S., Zhao, M., Chen, X., & Zhu, Y. (2023). StoneNet: An efficient lightweight model based on depthwise separable convolutions for kidney stone detection from CT images. *Interdisciplinary Sciences: Computational Life Sciences*, 15(4), 633−652. doi: 10.1007/s12539-023-00578-8

[19] Zhang, K., Bello, I.M., Su, Y., Wang, J., & Maryam, I. (2022). Multiscale depthwise separable convolution based network for high-resolution image segmentation. *International Journal of Remote Sensing*, 43(18), 6624−6643. doi: 10.1080/ 01431161.2022.2142081

[20] Pereira, J.L.J., Oliver, G.A., Francisco, M.B., Cunha Jr, S.S., & Gomes, G.F. (2022). A review of multi-objective optimization: Methods and algorithms in mechanical engineering problems. *Archives of Computational Methods in Engineering*, 29(4), 2285−2308. doi: 10.1007/s11831-021-09663-x

[21] Fallahnejad, R., Wanke, P.F., Mozaffari, M.R., & Tan, Y. (2024). A modification of double frontier ideal point method for Malmquist productivity index in the investigation of eco−innovation in transportation industry. *International Journal of Shipping and Transport Logistics*, 18(2), 191−222. doi: 10.1504/ IJSTL.2024.137894